Scaling of the Plasma Focus – Viewpoint from Dynamics

S.Lee
Nanyang Technology University, National Institute of Education
469, Bukit Timah Road, Singapore 259756

Abstract
The gross dynamics of the plasma focus is discussed in terms of phases. The dynamics of the axial and radial phases is computed using repectively a snowplow and an elongating slug model. A reflected shock phase follows, giving the maximum compression configuration of the plasma focus pinch. An expanded column phase is used to complete the post-focus electric current computation. Parameters of the gross focus pinch obtained from the computation, supplemented by experiments are summarised as follows:

		Deuterium	Neon (for SXR)
minimum radius	r_{min}	0.13a	0.04a
maximum length	z	0.7a	0.8a
radial shock transit	t_{comp}	$5x10^{-6}$a	$4x10^{-6}$a
pinch lifetime	t_p	$2x10^{-6}$a	$1x10^{-6}$a

where, for the times in sec, the value of anode radius, a, is in m. For the neon calculations radiative terms are included. The scaling suggests a speed enhancement effect on neutron yield, enhancing from the conventional I^4 to a superior I^8 scaling law.

Invited Paper International Workshop on Plasma Focus Research (PF 98), Kudowa, Poland July 1998

1. Introduction

This paper starts with a simple axial-radial model of the Mathers type plasma focus[1] to show that the elongating plasma focus pinch achieves a gross compressed configuration in which its minimum radius and its maximum length are dependent on its anode radius 'a'. Moreover for a given gas there appears to be experimental mechanisms that require the drive magnetic energy density to be constant over a range of the devices from small (kJ) to big (hundreds of kJ). From this it follows that the lifetime of the plasma focus pinch is also dependent on anode radius 'a'. Thus the bigger the anode radius, the bigger are the radius, length and lifetime of the compressed pinch. This dependence on 'a' is alone sufficient to derive the general rule that radiation yield is proportional to I^4. It also suggests a speed enhancement effect on neutron yield, which however does not appear to apply to soft x-ray (SXR) yield for microelectronics lithography.

2. Model

We use a snowplow model for the axial phase and a slug model for the radial pinch phase[2-4]. The end-point of compressions is fixed when the radially out-going reflected shock hits the in-going compressing piston.

2a. Axial phase:

We consider the rate of change of momentum of the current sheath sweeping up mass and equate this to the driving electromagnetic force (see Fig 1a).

$$\frac{d}{dt}\left[\pi\left(b^2-a^2\right)z\rho f_m\frac{dz}{dt}\right]=\frac{\mu f_c^2 I^2}{4\pi}\ln c \qquad (1)$$

*Invited paper to be presented at International Plasma Focus Symposium at Kudowa, Poland, July 1998

where b is the outer electrode radius, a the inner electrode radius, z the position of the 'snowplow' current sheath, ρ the ambient density, I the driving current, c=b/a, and μ the permeability of free space. The two parameters f_m and f_s are the mass swept-up factor and current factor used to account for the experimentally observed mass loss and current loss respectively [5].

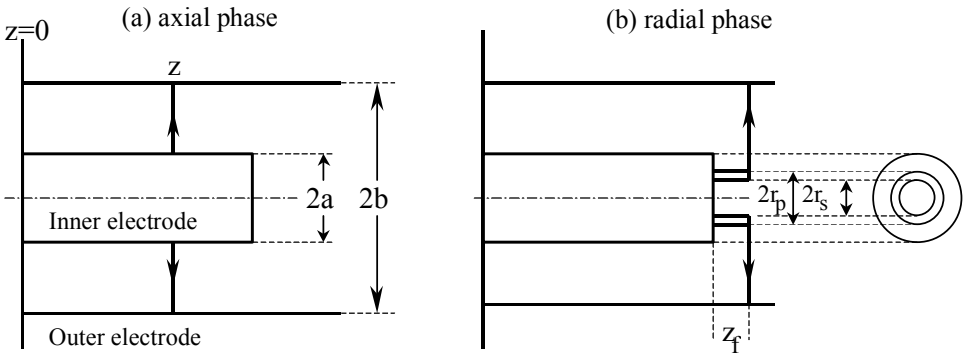

Fig 1: Schematic of (a) axial phase and (b) radial phase

The circuit equation which captures the effect of the changing inductance L_p, due to current sheath motion, on the current I is:

$$\frac{d}{dt}\left[\left(L_o + f_c L_p\right)I\right] = V_o - \frac{1}{C_o}\int_o^t I\,dt - r_o I \qquad (2)$$

where L_o, C_o and r_o are the fixed circuit inductance, capacitance and stray resistance, and L_p is:

$$L_p = \frac{\mu}{2\pi} z \ln c \qquad (3)$$

Equations (1) & (2) may be integrated step-by-step for the instantaneous values of I and z. Appropriate values used for f_m and f_c are found to be $f_m = 0.1$, $f_c = 0.7$.

2b. Radial Phase

In the radial phase (see Fig 1b), because of the compression configuration, less mass loss is observed so a radial mass swept-up factor f_{mr} is introduced. The current factor remains as f_c. We derive the shock speed from the driving magnetic pressure and use the same speed (except for a thermodynamic factor) for the elongation since the same magnetic pressure drives both the radial compression and axial elongation. We allow the current sheath (piston) to separate from the shock front by applying an adiabatic approximation[6]

relating a change in pressure P to a change in volume V, to a fixed mass of gas at any given instant of time t. These 3 equations are then closed with a fourth equation, this being the circuit equation. These equations are written as follows:

$$\frac{dr_s}{dt} = -\left\{\frac{\mu(\gamma+1)}{\rho f_{mr}}\right\}^{1/2} \frac{f_c I}{4\pi r_p} \tag{4}$$

$$\frac{dz_f}{dt} = -\frac{2}{\gamma+1}\frac{dr_s}{dt} \tag{5}$$

$$\frac{dr_p}{dt} = \frac{\frac{2}{\gamma+1}\left(\frac{r_s}{r_p}\right)\frac{dr_s}{dt} - \frac{r_p}{\gamma I}\left(1-\frac{r_s^2}{r_p^2}\right)\frac{dI}{dt} - \frac{1}{\gamma+1}\frac{r_p}{z_f}\left(1-\frac{r_s^2}{r_p^2}\right)\frac{dz_f}{dt}}{\frac{\gamma-1}{\gamma}+\frac{1}{\gamma}\frac{r_s^r}{r_p^2}} \tag{6}$$

$$\frac{d}{dt}\left[(L_o + f_c L_p)I\right] = V_o - \frac{1}{C_o}\int I dt - r_o I \tag{7}$$

where in the radial phase

$$L_p = \frac{\mu}{2\pi} z_o \ln c + \frac{\mu}{2\pi} z_f \ln\left(\frac{b}{r_p}\right) \tag{7a}$$

The four equations (4) – (7) may be integrated step-by-step for the instantaneous values of r_s, r_p,z_f & I. For deuterium, γ is taken as 5/3. This phase is completed when the shock front hits the axis i.e. $r_s = 0$ with velocity $(dr_s/dt)_{on\text{-}axis}$.

2c. Reflected Shock Phase

When the shock front hits the axis, because the focus plasma is collisional, a reflected shock develops (position r_r) which moves radially outwards, whilst the radial current sheath piston continues to move inwards (see Fig 2).

This phase is simulated with the following equations:

$$\frac{dr_r}{dt} = f_{RS}\left(\frac{dr_s}{dt}\right)_{on-axis} \tag{8}$$

where we usually take f_{rs} as 0.3 empirically.

$$\frac{dz_f}{dt} = -\frac{2}{\gamma+1}\left(\frac{dr_s}{dt}\right)_{on-axis} \qquad (9)$$

$$\frac{dr_p}{dt} = -\frac{r_p}{\gamma I}\left(1-\frac{r_r^2}{r_p^2}\right)\frac{dI}{dt} - \frac{1}{\gamma+1}\frac{r_p}{z_f}\left(1-\frac{r_r^2}{r_p^2}\right)\frac{dz_f}{dt} \Bigg/ \frac{\gamma-1}{\gamma} + \frac{1}{\gamma}\left(\frac{r_r}{r_p}\right)^2 \qquad (10)$$

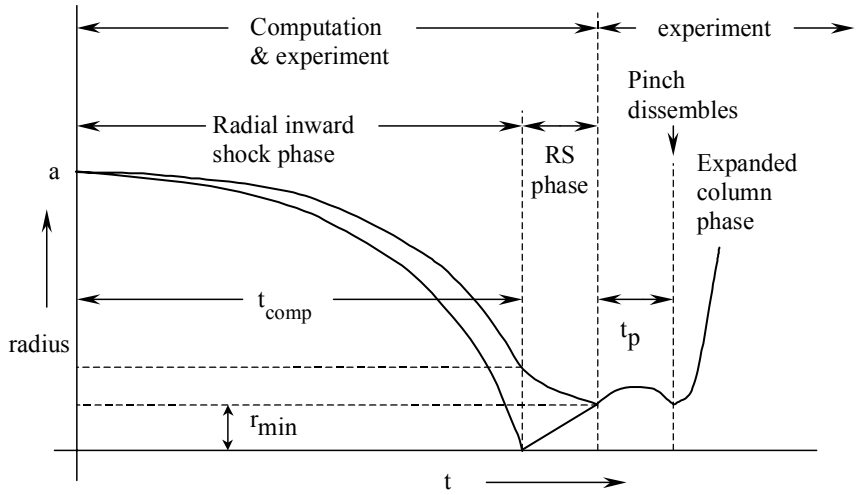

Fig 2. Schematic of radial phases

The circuit equations may be used unchanged from (7) supplemented by (7a). Equations (8), (9), (10) and (7) may be integrated step-by-step for r_r, z_f, r_p and I.

When the out-going reflected shock hits the in-going piston the compression enters a radiative phase in which for gases such as neon e.g. radiation cooling may actually enhance the compression. For deuterium we assume the radiative phase is not significant to the dynamics. We treat this point as the point of maximum compression with minimum gross radius r_{min} and maximum plasma pinch length z_p. If we just want the gross parameters of the plasma focus pinch the calculations may end here.

2d. Expanded Column Phase

To simulate the current trace beyond this point we allow the column to suddenly attain the radius of the anode, and use the expanded column inductance for further integration.

3. Normalization:

The equations are normalised in the following manner [2-4]:

$$\tau = \frac{t}{t_o}, \quad \zeta = \frac{z}{z_o}, \quad \iota = \frac{I}{I_o}, \quad \delta = \frac{r_o}{Z_o} \quad \text{where } Z_o = \sqrt{\frac{L_o}{C_o}}$$

$$\kappa_s = \frac{r_s}{a}, \quad \kappa_p = \frac{r_p}{a}, \quad \zeta_f = \frac{z_f}{a}$$

$$t_o = \sqrt{L_o C_o} \text{ and } I_o = V_o / Z_o$$

Axial Phase:

The normalized axial phase equations are:

$$\frac{d^2\zeta}{d\tau^2} = \frac{\alpha^2\iota^2 - \left(\frac{d\zeta}{d\tau}\right)^2}{\zeta} \tag{11}$$

$$\frac{d\iota}{d\tau} = \frac{1 - \int \iota d\tau - f_c\beta\frac{d\zeta}{d\tau}\iota - \delta\iota}{1 + f_c\beta\zeta} \tag{12}$$

to compute ϕ and ι; with two scaling parameters:

$$\beta = \left[\frac{\mu}{2\pi} z_o \ln c\right] / L_o$$

which is the ratio of the full axial phase tube inductance to the external fixed inductance. Ratio of characteristic electrical discharge time to characteristic axial transit times is:

$$\alpha = t_o / t_a$$

$$\text{where} \quad t_a = \left[\frac{4\pi^2\left(c^2 - 1\right)}{\mu \ln c}\right]^{1/2} \frac{z_o\sqrt{f_m}}{f_c} \frac{\sqrt{\rho}}{\left(I_o / a\right)}$$

giving a characteristic axial transit speed of $v_a = z_o/t_a$ of

$$v_a = \left[\frac{\mu \ln c}{4\pi^2\left(c^2 - 1\right)}\right]^{1/2} \frac{f_c}{\sqrt{f_m}} \frac{\left(I_o / a\right)}{\sqrt{\rho}} \tag{13}$$

We note the dependence of v_a on $(I_o/a)/\sqrt{\rho}$ which is designated as the drive parameter S.

Radial Phase

Normalised radial phase equations are:

$$\frac{d\kappa_s}{d\tau} = -\alpha\alpha_1 \frac{\iota}{\kappa_p} \tag{14}$$

$$\frac{d\zeta_f}{d\tau} = -\frac{2}{\gamma+1}\frac{d\kappa_s}{d\tau} \tag{15}$$

$$\frac{d\kappa_p}{d\tau} = \frac{\frac{2}{\gamma+1}\frac{\kappa_s}{\kappa_p}\frac{d\kappa_s}{d\tau} - \frac{\kappa_p}{\gamma\iota}\left(1-\frac{\kappa_s^2}{\kappa_p{}^2}\right)\frac{d\iota}{d\tau} - \frac{1}{\gamma+1}\frac{\kappa_p}{\zeta_f}\left(1-\frac{\kappa_s^2}{\kappa_p^2}\right)\frac{d\zeta_f}{d\tau}}{\frac{\gamma-1}{\gamma}+\frac{1}{\gamma}\frac{\kappa_s^2}{\kappa_p^2}} \tag{16}$$

$$\frac{d\iota}{d\tau} = \frac{1-\int \iota d\tau + \frac{\beta_1}{F} f_c \frac{\zeta_f}{\kappa_p}\frac{d\kappa_p}{d\tau}\iota + \frac{\beta_1}{F} f_c \ln(\frac{\kappa_p}{c})\frac{d\zeta_f}{d\tau}\iota - \delta\iota}{1+f_c\beta - f_c\frac{\beta_1}{F}\zeta_f \ln\left(\frac{\kappa_p}{c}\right)} \tag{17}$$

where $\beta_1 = \frac{\beta}{\ln c}$, $F = \frac{z_o}{a}$

and the ratio of the characteristic axial transit time to characteristic pinch time

$$\alpha_1 = \frac{t_a}{t_p} = \left[(\gamma+1)(c^2-1)\right]^{1/2}\frac{F\sqrt{f_m}}{2\sqrt{\ln c}}$$

Hence $t_p = \frac{4\pi}{[\mu(\gamma+1)]^{1/2}}\frac{\sqrt{f_{mr}}}{f_c}\frac{\sqrt{\rho}}{(I_0/a)}a$

and characteristic pinch time a/t_p is

$$v_p = \frac{[\mu(\gamma+1)]}{4\pi} f_c \frac{I_o/a}{\sqrt{\rho}} \tag{18}$$

We note that v_p has the same dependence on drive parameter S as V_a.

4. Parameters and Scaling

The UNU/ICTP PFF is a 3 kJ plasma focus [7] designated as the United National University/International Centre for Theoretical Physics Plasma Focus Facility. This device was developed during UNU/ICTP training programmes and is now established in

6 countries for postgraduate training and research. To compute the above model for the UNU/ICTP PFF we note its operational parameters:

$C_o = 3 \times 10^{-5}$F $\quad L_o = 1.1 \times 10^{-7}$H
$a = 0.95 \times 10^{-2}$m $\quad b = 3.2 \times 10^{-2}$m $\quad z_o = 0.16$m
$c = 3.37 \quad F = 16.84$
Hence $t_o = \sqrt{L_o C_o} = 1{,}82 \times 10_s^{-6} \quad Z_o = \sqrt{L_o / C_o} = 0.06\Omega$

Typical operation is at 14 kV with ambient pressure of 3.5 torr deuterium giving:

$\rho = 8.2 \times 10^{-4}$ kgm^{-3} $\quad V_o = 1.4 \times 10^4$ $\quad$ Also r_o –0.012Ω
Hence $I_o = V_o/Z_o = 2.33 \times 10^5$A $\quad \delta = r_o/Z_o = 0.2$
we take $f_c = 0.7 \quad f_m = 0.1$
f_{mr}=0.3
Hence $t_a = 1.38 \times 10^{-6}$s $\quad v_a = 1.15 \times 10^5$m/s
$t_p = 6..0 \times 10^{-8}$s $\quad v_p = 1.6 \times 10^5$m/s

Hence
$\alpha = 1.31 \quad \alpha_1 = 23.2$
$\beta = 0.35 \quad \beta_1 = 0.29$

We also use $\gamma = 5/3$ (specific heat ratio for fully ionized deuterium)

The above values of α, β, δ, f_c, f_m are used with equations (11) and (12) to compute the axial phase dynamics for ι and ς . For the radial phase dynamics additional parameters from the above list namely, α_1, γ, β_1, F, c are used together with the 4 equations 14 – 17 to compute the radial phase dynamics for κ_s, κ_p, ζ_f and ι. In the reflected shock phase we take the reflected shock speed ratio $f_{rs} = \underline{0.3}$.

Even without numerical computation, the normalization of the axial and radial phases equations has shown us the following regarding the characteristic times and speeds. We note that in the design of plasma focus devices the geometrical ratio c is between 2 and 3 so that the factor $[(c^2\text{-}1)/\ln c)]^{1/2}$ remains within a small range. Thus basically: $t_a \sim z_o/S$ and $t_p \sim a/S$ and both the axial and radial speeds v_a and v_p are proportional to the drive parameter S.

Over a range of machines, from small to big, it is experimentally observed that the drive parameter is constant for neutron optimized operation in deuterium. This is consistent with observed constant speed over the range of devices. Hence the characteristic times scale with dimension z_o for the axial phase and 'a' for the radial phase.

Moreover it is implied in the equations 14-16 that at any point in the radial trajectory the values of r_s, r_p and z_f are proportional to 'a'. Hence in the position of maximum compression, which gives the minimum radius r_{min} of the piston position, the gross parameters r_{min} and z_p are both proportional to anode radius 'a'.

5. Results of computation and discussion.

Computation for the trajectories and electric current yield the following results. Fig 3 shows the axial phase dynamics in terms of axial position and speed presented in real quantities. It shows that the current sheath reaches the end of the axial phase at 2.87 μs with a peak speed of 8.6 cm/μs.

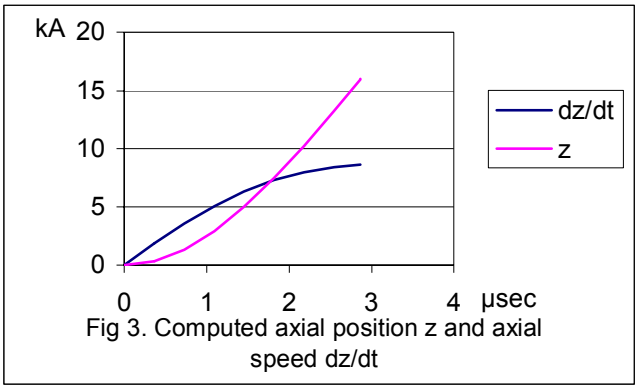

Fig 3. Computed axial position z and axial speed dz/dt

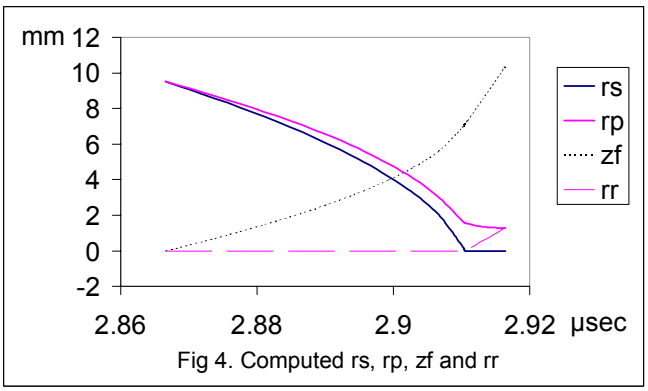

Fig 4. Computed rs, rp, zf and rr

Figure 4 shows the radial phase dynamics. The shock front and the piston start together at r=a; the length of the focus pinch is zero at this time. The shock front accelerates onto the axis, hitting the axis 40 ns from the start of the radial phase. At this time the piston position is 1.6mm from the axis and the length of the lengthening focus column is 7.1 mm. According to this computation the speed of the on-axis shock front exceeds 50 cm/μs. The piston speed, which had peaked at 30 cm/μs, reduces sharply as the shock approaches the axis. We note the limitation of the radial model as follows.

Implicit in this radial model is the assumption of instantaneous communication between the piston and the shock front ie an assumption of infinite signal speed. This assumption results in the computed speeds being too high. If we consider the actual communication delay due to the finite small disturbance speed between the piston and shock front (of the order of ns, dependent on plasma slug temperature) the shock front would at any instant feel the considerably smaller pressure of the piston at an earlier time, and likewise the piston would feel the effect of the shock front moving at a slower speed at an earlier

position. This delay effect incorporated into the model, would considerably slow down both the shock front and piston, as they near the axis, to peak values of 25-30 cm/μs for the shock front on-axis and to about 20 cm/μs a short time before the shock front hits the axis. As the reduction in speeds is only significant near the axis (final 3 mm of shock front travel) the shock transit time is increased only slightly.

When the shock front hits the axis, a reflected shock develops and moves radially outwards. The piston continues to compress inwards until it hits the out-going reflected shock front. We define this point where the piston meets the reflected shock as the point of maximum gross compression, and label this radial position r_{min}. Experimental observations using shadowgraphs complemented by electrical and x-ray measurements, indicate that beyond this point of time the plasma radius remains at about the value of r_{min} for a short period (some 20ns for the UNU/ICTP PFF) before the pinch dissembles rather violently. For deuterium this model is not extended specifically to compute the dynamics of this phase. For neon we have included this as a radiative phase, adding radiative terms into the computation. Indeed for neon, the radiative terms are energetically significant and even affect the dynamics to give evidence of further compression due to radiative cooling..

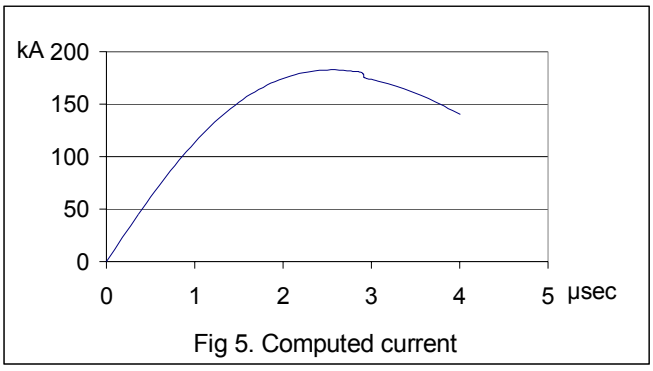

Fig 5. Computed current

Figure 5 shows the computation of the electric current. This computation was extended to the post-focus phase by using a simple expanded column approximation. The current agrees well with experimentally observed Rogowskii coil measurements.

The key computed pinch parameters for the deuterium focus are as follows:

$$r_{min} = 0.13\ a \quad (18)$$

$$z_p = 0.7\ a \quad (19)$$

$$t_{comp} = 5 \times 10^{-6}\ a \quad (20)$$

We have not computed t_p but this has been measured experimentally as [8]:

$$t_p = 2 \times 10^{-6}\ a \quad (21)$$

The above results have been verified experimentally[8,13] with shadowgraphs and measurements of current, voltage, neutron and SXR of the UNU/ICTP PFF operated in deuterium.

6. Scaling of Yield

For a thermalised plasma we can generally assign density n and temperature T. If the particles of density n interact among themselves with a cross section C(T), generally depended on T, we may write down a general radiation yield, Y, relationship as follows:

$$Y \sim n^2 \text{ (volume) (lifetime) } C \qquad (22)$$

For the plasma focus, given the dimensional and temporal dependence as shown in equations (18), (19) and (21) we have

$$Y \sim n^2 a^4 C \qquad (23)$$

6a. Constant S operation

A survey of plasma focus devices have shown that in deuterium the drive parameter [8] is S = 90 kA per cm per $(\text{torr})^{½}$ of deuterium over a range large range of energy from 3kJ – 200kJ. This corresponds to the well-know phenomenon that similar speeds are observed in small devices as well as in large devices. For example the peak axial speeds for neutron-optimised operation is experimentally observed to be 8 – 10 cm/μs. This has also been expressed as an average axial speed of 5-5.5 cm/μs. Similarly the radial speeds peak at 25-30 cm/μs for all devices, big or small. This peak speed occurs as the radial in-going shock goes on-axis. Such constant speeds observed over such a range of device energies indicate that at any point of the plasma focus operation, e.g. end of axial phase or end of inward shock phase as the inward radial shock goes on axis, the temperature in a small focus is the same as the temperature in a big focus. By extension it is inferred that the temperature at the point of maximum compression is also the same for a small focus as for a big focus. This is of course consistent from the viewpoint of energy densities. The quantity S is the magnetic energy density driving the system. Hence since the driving magnet energy is constant over the range of devices, it is consistent that the temperatures generated is also constant over the range of devices.

Given this observed constancy we have:

$$\frac{(I/a)}{\rho^{1/2}} = \text{constant} \qquad (24)$$

$$\text{Hence } I \sim a\rho^{1/2} \qquad (25)$$

For a deuterium focus, the pinched gas is fully ionised and the number density of deuterium ions in the pinch is proportional to the ambient density ρ.

Hence applying equation (25) to Eq (23) and noting that since T=constant over the range of devices, the cross section C is also constant and we have[9]:

$$Y \sim I^4 \qquad (26)$$

This yield law really applies to the thermonuclear neutron yield. Experimentally for a small neutron-optimised plasma focus it has been shown [10] that the thermonuclear

component of the neutron yield is only 15%, the other 85% being ascribed to beam-target mechanisms. Nevertheless we note that these yield proportions are occurring at a plasma ion temperature of about 1 keV and a beam energy of about 50 keV.

6b. Speed-enhancement of neutron yield

This leads to the concept of speed enhancement [9,12]. If the driver parameter S is increased, the drive energy density increases, the speed increases and we may expect the focus pinch ion temperature also to increase. This leads to a dramatic increase in neutron yield since in the range of 1 – 10 keV, the neutron fusion cross-section is a rapid function of T with $C \sim T^n$ n being greater than 4. And since $T \sim v^2$, if we keep 'a' constant as the drive current is increased, we increase the drive parameter S. This will give us a thermonuclear yield component better than

$$Y \sim I^8 \qquad (27)$$

Increase in speed will also increase the energy of the beam component. The beam component will however not have a significant increase since above 50 keV the cross section C barely increases with T. This means that as operational speed is increased, the plasma focus neutron yield becomes more thermonuclear. For example an increase in speed by 20% increases the focus pinch temperature by more than 40%, with the thermonuclear yield increasing by more than 5 times, whilst the beam-target component barely increases. This means that even a 20% increase in the drive parameter for the UNU/ICTP PFF could not only significantly increase its neutron but also make this yield predominantly thermonuclear.

However it is not a simple matter to increase the drive speed. Experiments have shown that if the peak axial speed is pushed above 10 cm/μs, plasma focus quality simply deteriorates. A force-field flow-field decoupling mechanism [3] has been proposed to account for the deterioration of the focus quality. According to shock theory for a gas with specific heat ratio of 5/3, the contact surface or piston should separate from the shock front 1 cm for every 4 cm travelled by the shock front. At lower speeds, although deuterium is already fully ionised at 4 cm/μs, there is still considerable diffusion of the magnetic field into the plasma all the way to the shock front so that effectively the centre of drive force field is not significantly behind the centre of the mass field. However at a speed above 9 or 10 cm/μs, the electrical conductivity is sufficient to limit the field penetration resulting in a separation of the centre of the force field from the centre of the mass field. This separation grows with distance travelled. If this separation becomes of the order of the anode radius, then when the shock wave sweeps around the anode in the radial compression, the piston is still travelling axially a radius away and when the shock hits the axis the piston may still not have started its radial compression. Such a compression will be weak. It is postulated that this force-mass decoupling mechanism[3,11] becomes significant above the 'speed-limit' of 9-10 cm/μs observed for deuterium focus operation.

An experiment[12,13] was carried out to achieve this speed increase yet overcome the decoupling by keeping the 'speed-enhanced' region short. A stepped-anode was used

consisting of a 'normal' radius section designed with the normal S value, followed by a short 'speed-enhanced' section for which the S value was increased by a reduction of 'a'. By this means speeds up to 15cm/μs was achieved with focussing. Neutron-yield enhancement was indicated.

However this experiment was severely limited in its scope since 'speed-enhancement' was achieved not by an increase of I at fixed 'a', rather by effectively fixing I and reducing 'a'. This was due to the limitations imposed by the UNU/ICTP PFF in its electrical range of operation. It is proposed that speed-enhancement experiments should be carried out in a machine with fixed 'normal' 'a'; and to increase I above 'normal' values.

6c Scaling for neon operation

The plasma focus is operated in neon to generate SXR in the wavelength range[17] of 0.8 – 1.4 nm. This wavelength range is found suitable for microelectronics lithography[14] from the point of view of near optimum contrast using existing mask technology. We have performed calculations[15,16] using the axial-radial model described above but including radiation terms (free-free, free-bound and bound-bound) into the dynamical equations as well as SXR yield equations. These calculations indicate that the focus pinch temperature needs to be adjusted to 300 – 400 eV for optimum yield in the correct wavelength range which arises from He-like and H-like Neon ions. We have selected 350 eV which corresponds to an axial speed of 4.5 cm/μs. For the UNU/ICTP PFF we found that optimum yield is obtained at 14 kV operation when an ambient pressure of 1 torr is used. Because the neon is still ionising (rather than fully ionised) its effective specific heat ratio may be approximated as 1.4. This gives it a thinner slug layer and a smaller compressed radius. Some of the parameters of the neon focus pinch are calculated as:

$$r_{min} = 0.04a$$
$$z_{max} = 0.8a$$
$$t_{comp} = 4x10^{-6}a$$

These agree with experimental observations. We have also estimated from experiments:

$$t_p = 1x10^{-6}a$$

Since the pinch temperature needs to be fixed at 350 eV no speed-enhancement is possible for the neon focus operated for microelectronics lithography purposes.

7. Conclusion

We conclude from computation, supplemented by experimental observations that the plasma focus pinch has gross parameters that scale according to anode radius 'a' in the following manner:

		Neon (for SXR)	Deuterium
minimum radius	r_{min}	0.13a	0.04a
maximum length	z	0.7a	0.8a
radial shock transit	t_{comp}	$5x10^{-6}$a	$4x10^{-6}$a
pinch lifetime	t_p	$2x10^{-6}$a	$1x10^{-6}$a

where, the times are in sec, when the value of anode radius, a, is in m.

References

1 J.W.Mathers, Phys Fluids Supple, **7**, 5(1964)

2. S Lee et al "Technology of the Plasma Focus" in *Laser and Plasma Technology*, Ed by S Lee et al, World Sci Pub Co, Singapore (1985) p387-420

3. S Lee "Technology of a small plasma focus-incorporating some experience with the UNU/ICTP PFF" in *Small Plasma Physics Experiments*, Ed S Lee & P H Sakanaka, World Sci Pub Co (1989) p113-169

4. S Lee, IEEE Trans Plasma Sci **19**, 912-919 (1991)

6. S P Chow, S Lee & B C Tan, J Plasma Phys **8**, 21-31 (1972)

6. D E Potter, Phys Fluids **14**, 1911 (1971)

7. S Lee et al, Amer J Phys **56**, 62 (1988)

8. S Lee & A Serban, IEEE Trans Plasma Sci **24**, 1101-1105 (1996)

9. S Lee, "Sharing of Fusion related Technology among Developing Countries" in *Fusion Energy and Plasma Physics*, Ed P H Sakanaka, World Sci Pub Co (1988) p754-774

10. S P Moo, C K Chakrabarty & S Lee , IEEE Trans Plasma Sci **19**, 515-519 (1991)

11. K H Kwek, T Y Tou & S Lee, IEEE Trans on Instru & Meas **IM-38**, 103 (1989)

12. S Lee & A Serban, "Speed –enhanced Neutron Yield in Plasma Focus", International Conf on Plasma Phys, Foz do Iguassu, Brazil, Oct 1994, Conference Procs Vol 1, p181-184

13. A Serban, "Anode Geometry & Focus Characteristics" PhD thesis, Nanyang Technological Uni (1995)

14. S Lee et al, "High Rep Rate High Performance Plasma Focus as a Powerful Radiation Source" accepted to be published in IEEE Trans Plasma Sci 1998

15. M H Liu "Soft X-rays from Compact Plasma Focus", PhD thesis, Nanyang Technological Uni (1997)

16. M H Liu and S Lee "SXR Radiation Modelling for Neon Plasma Focus" presented at 1998 International Congress on Plasma Physics, Prague, Czech Republic, July 1998.

17. M H Liu, X P Feng, S.V. Springham & S Lee, "Soft X-ray Yield Measurement in a Small Plasma Focus Operated in Neon", IEEE Trans Plasma Sci. **26**(2), 135-140 (1998)